The Astrophysical Journal, 613:1143–1156, 2004 October 1

MASSIVE BLACK HOLES IN STAR CLUSTERS. II. REALISTIC CLUSTER MODELS

Holger Baumgardt,[1] Junichiro Makino,[2] and Toshikazu Ebisuzaki[1]

Received 2004 March 15; accepted 2004 June 4

ABSTRACT

We have followed the evolution of multimass star clusters containing massive central black holes through collisional N-body simulations done on GRAPE6. Each cluster is composed of between 16,384 and 131,072 stars together with a black hole with an initial mass of $M_{\rm BH} = 1000\ M_{\odot}$. We follow the evolution of the clusters under the combined influence of two-body relaxation, stellar mass loss, and tidal disruption of stars by the massive central black hole. We find that the (three-dimensional) mass density profile follows a power-law distribution $\rho \sim r^{-\alpha}$ with slope $\alpha = 1.55$ inside the sphere of influence of the central black hole. This leads to a constant-density profile of bright stars in projection, which makes it highly unlikely that core-collapse clusters contain intermediate-mass black holes (IMBHs). Instead, globular clusters containing massive central black holes can be fitted with standard King profiles. Because of energy generation in the cusp, star clusters with IMBHs expand. The cluster expansion is so strong that clusters that start very concentrated can end up among the least dense clusters. The amount of mass segregation in the core is also smaller compared to postcollapse clusters without IMBHs. Most stellar mass black holes with masses $M_{\rm BH} > 5\ M_{\odot}$ are lost from the clusters within a few gigayears through mutual encounters in the cusp around the IMBH. Black holes in star clusters disrupt mainly main-sequence stars and giants and no neutron stars. The disruption rates are too small to form an IMBH out of a $M_{\rm BH} \approx 50\ M_{\odot}$ progenitor black hole even if all material from disrupted stars is accreted onto the black hole, unless star clusters start with central densities significantly higher than what is seen in present-day globular clusters. We also discuss the possible detection mechanisms for IMBHs. Our simulations show that kinematical studies can reveal 1000 $M_{\odot}$ IMBHs in the closest clusters. IMBHs in globular clusters are weak X-ray sources, since the tidal disruption rate of stars is low and the star closest to the IMBH is normally another black hole, which prevents other stars from undergoing stable mass transfer. For globular clusters, dynamical evolution can push compact stars near the IMBH to distances small enough that they become detectable sources of gravitational radiation. If 10% of all globular clusters contain IMBHs, extragalactic globular clusters could be one of the major sources of gravitational wave events for *LISA*.

Subject headings: black hole physics — globular clusters: general — methods: n-body simulations — stellar dynamics

Online material: color figures

1. INTRODUCTION

This is the second paper in a series of N-body simulations that deal with the dynamical evolution of star clusters containing massive central black holes (BHs). In Baumgardt et al. (2004, hereafter Paper I), we followed the evolution of single-mass clusters with BHs that contained a few percent of the total system mass. We showed that the density distribution of stars inside the sphere of influence of the BH follows a $\rho \sim r^{-1.75}$ power law, in good agreement with results from previous analytical estimates and indirect simulation methods (Bahcall & Wolf 1976; Cohn & Kulsrud 1978; Marchant & Shapiro 1980). We also derived the rate of tidal disruption of stars. The present paper extends these results to the more realistic but much less studied case of a star cluster with a spectrum of stellar masses and is aimed at globular clusters with intermediate-mass black holes (IMBHs) of a few hundred to a few thousand solar masses at their centers.

X-ray observations of starburst and interacting galaxies have revealed a class of ultraluminous X-ray sources (ULX) whose luminosities exceed the Eddington luminosities of stellar-mass BHs by orders of magnitude (Makishima et al. 2000), making them good candidates for IMBHs. The irregular galaxy M82, for example, hosts a ULX with luminosity $L > 10^{40}$ ergs s^{-1} near its center (Matsumoto et al. 2001; Kaaret et al. 2001), the position of which coincides with that of the young ($T \approx 10$ Myr) star cluster MGG-11. Portegies Zwart et al. (2004) have performed N-body simulations of several star clusters in M82, using the cluster parameters determined by McCrady et al. (2003). They found that runaway merging of massive stars could have led to the formation of an IMBH with a few hundred to a few thousand solar masses in MGG-11, thereby explaining the presence of the ultraluminous X-ray source. General conditions in which runaway merging of stars can lead to the formation of IMBHs were discussed in Portegies Zwart & McMillan (2002) and Rasio et al. (2004).

Apart from runaway collisions of main-sequence stars, massive BHs could also be built up through the merger of stellar-mass BHs (Mouri & Taniguchi 2002) via gravitational radiation in dense enough star clusters. In less concentrated clusters this process is also possible, but may take up to a Hubble time (Miller & Hamilton 2002). Finally, IMBHs could also form by the accretion onto a stellar-mass BH of interstellar cluster gas as a result of radiation drag from bright stars, provided the stellar mass function of the cluster is shallow enough (Kawakatu & Umemura 2004).

[1] Astrophysical Computing Center, RIKEN, 2-1 Hirosawa, Wako-shi, Saitama 351-0198, Japan.
[2] Department of Astronomy, University of Tokyo, 7-3-1 Hongo, Bunkyo-ku, Tokyo 113-0033, Japan.

Although there are several possible ways to form IMBHs, the observational evidence for intermediate-mass BHs in star clusters is as yet much less clear. Because of their high central densities and since they are relatively close, Galactic core-collapse clusters are obvious places to look for IMBHs. Indeed, for almost 30 yr M15 has been thought to harbor an IMBH in its center (Newell et al. 1976). The most recent analysis of this cluster was done by Gerssen et al. (2002, 2003), who used the *Hubble Space Telescope* (*HST*) to obtain new spectra of stars in the central cluster region. They found that the velocity dispersion can best be explained by an IMBH of mass $(1.7 \pm 2.7) \times 10^3\ M_\odot$. However, Baumgardt et al. (2003a) have shown that the observational data can also be explained by the core-collapse profile of a "standard" star cluster without a massive central BH. In this case, the central rise of the mass-to-light ratio is created by an unseen concentration of neutron stars and high-mass white dwarfs. Such a model is also able to explain the velocity dispersion derived from the proper motion of stars near the center of M15 (McNamara et al. 2003, 2004). Similarly, a dense concentration of compact remnants might also be responsible for the high mass-to-light ratio of the central region of NGC 6752 seen in pulsar timings (Ferraro et al. 2003; Colpi et al. 2003). Outside our own galaxy, Gebhardt et al. (2002) have reported evidence for a $20,000\ M_\odot$ BH in the M31 globular cluster G1, but Baumgardt et al. (2003b) showed that dynamical simulations without BHs completely explain the observed velocity dispersion and density profile of this cluster.

Despite the unclear observational situation, the presence of IMBHs in star clusters remains an interesting possibility. They would provide the missing link between the stellar mass BHs that form as a result of stellar evolution and the supermassive BHs in galactic centers (Ebisuzaki et al. 2001). They would also be prime targets for the forthcoming generation of both ground- and space-based gravitational wave detectors owing to their high masses and the fact that they have the potential to merge with other BHs if residing in dense star clusters.

In this paper we study the dynamical behavior of massive BHs in globular clusters. Section 2 describes the setup of our runs, and in § 3 we present our main results concerning the dynamical evolution of the star clusters, the tidal disruption of stars, and the possibilities of detecting the central BH. In § 4 we report our conclusions.

2. DESCRIPTION OF THE RUNS

We simulated the evolution of clusters containing between $N = 16,384$ and 131,072 (128K) stars using Aarseth's collisional *N*-body code NBODY4 (Aarseth 1999) on the GRAPE6 computers of Tokyo University (Makino et al. 2003). Most clusters were treated as isolated and followed King $W_0 = 7.0$ profiles initially. Simulations were run for a Hubble time, which was assumed to be $T = 12$ Gyr. Since BHs probably form early on in the evolution of a globular cluster, e.g., by runaway merging of massive stars, we started our runs with a massive BH at rest at the cluster center. As in Paper I, we modified the velocities of the cluster stars to prevent the cluster center from collapsing after adding the IMBH to the cluster.

All clusters started with a central BH of mass $M_{\rm BH} = 1000\ M_\odot$. If the $M_\odot$-σ relation found by Gebhardt et al. (2000) for galactic bulges holds for globular clusters as well, this corresponds to the IMBH mass expected in a typical globular cluster. In addition, the best case found so far for an IMBH in a star cluster, M82 X-1 in MGG-11, must have a mass between a few hundred to a few thousand solar masses based on its X-ray luminosity and the frequency of quasi-periodic oscillations seen in the X-ray flux (Matsumoto et al. 2001; Strohmayer & Mushotzky 2003).

Stellar evolution was treated by the fitting formulae of Hurley et al. (2000), assuming a mean cluster metallicity of $Z = 0.001$ and a neutron star retention fraction of 15%. The 15% retention fraction was imposed by immediately removing 85% of all neutron stars at the time of their formation while leaving the velocities of the remaining ones unchanged. The exact form of the initial mass function (IMF) at the low-mass end will not critically influence the results of our simulations, since such stars are mere test particles in the gravitational field of the higher mass stars. More important is the mass function at the high-mass end, especially the number and mass distribution of BHs formed during the run. Unfortunately, the initial-to-final mass relation for high-mass stars is currently not precisely known, since it depends among other things on the assumed amount of stellar wind mass loss in the final phases of stellar evolution and the details of the explosion mechanism (Fryer & Kalogera 2001). In addition, the metallicity of the progenitor star will affect the mass of the final BH (Heger et al. 2003) for low-metallicity stars, so globular clusters with different metallicities might have different BH mass distributions. Since the fraction and mass distribution of high-mass BHs could have a strong influence on the outcome of our simulations, we performed two series of simulations.

In our first series of simulations, the mass function of the cluster stars was given by a Kroupa (2001) IMF with a lower mass limit of $0.1\ M_\odot$ and an upper mass limit of $30\ M_\odot$. Since this upper mass limit is only slightly above the mass at which BHs instead of neutron stars form in stellar evolution, these clusters contain only a small fraction of stellar mass BHs, all of them with masses below $3\ M_\odot$. In the second series of simulations we used an upper mass limit of $100\ M_\odot$ and transformed the stars directly into BHs without further mass loss. In this series, the BHs of highest mass formed have $\sim 45\ M_\odot$. In both types of simulations, all BHs were retained in the clusters. These two cases are the most extreme models, and most likely real globular clusters fall in between.

We did not include a primordial binary population. The presence of a primordial binary population might help the formation of IMBH through enhancing the stellar collisions (e.g., Fregeau et al. 2003). Its effect on the structure of a cluster with central IMBH would be to decrease the central density through hardening. Thus, our present result without primordial binaries gives the upper limit of the central density.

Stars were assumed to be tidally disrupted if their distance to the central BH was smaller than the critical distance given by equation (3.2) in Kochanek (1992):

$$r_t = 1.3 \left(\frac{M_{\rm BH}}{2M_*} \right)^{1/3} R_*, \tag{1}$$

where $M_{\rm BH}$ and M_* are the masses of the BH and the star, respectively, and R_* is the stellar radius. The stellar radii were taken from the formulae of Hurley et al. (2000). The mass of tidally disrupted stars was added to the mass of the central BH. So far we have not incorporated the effects of gravitational radiation in our runs, since the central densities reached in our simulations are not large enough that gravitational radiation becomes important. We also did not include stellar collisions, which become dynamically important when the velocity dispersion around the BH becomes equal to the

TABLE 1
DETAILS OF THE PERFORMED N-BODY RUNS

N	$N_{\rm sim}$	W_0	$M_{\rm up}$ ($M_\odot$)	$M_{\rm Cl}$[a] ($M_\odot$)	$r_{h,i}$ (pc)	$r_{h,f}$[a] (pc)	$M_{{\rm BH},i}$ ($M_\odot$)	$M_{{\rm BH},f}$[a] ($M_\odot$)	$N_{\rm Tid}$[a]
16384.....	4	7.0	30.0	9778.5	4.87	28.06	1000.0	1007.2	8
32768.....	2	7.0	30.0	18809.5	4.87	21.97	1000.0	1023.7	19
65536.....	1	7.0	30.0	39310.9	4.87	17.33	1000.0	1030.3	27
131072.....	1	7.0	30.0	76936.8	4.87	13.98	1000.0	1045.5	37
32768.....	2	7.0	100.0	20681.2	4.87	27.39	1000.0	1003.3	2
65536.....	1	7.0	100.0	41024.1	3.86	18.97	1000.0	1001.9	5
131072.....	1	7.0	100.0	83919.4	3.07	14.00	1000.0	1004.4	11
16384.....	2	7.0	30.0	9739.6	0.79	32.06	1000.0	1039.9	24
16384.....	2	10.0	30.0	9868.9	6.23	29.40	1000.0	1015.8	12

[a] For clusters with more than one simulation, parameters given are average values.

escape velocity from the stellar surface, since stars can no longer undergo large-angle encounters (Frank & Rees 1976). Even for main-sequence stars, this corresponds to distances of $r_{\rm coll} = 10^{-5}$ pc from the BH, which is far inside the distance of the innermost stars from the IMBH.

Table 1 gives an overview of the simulations performed. It shows the number of cluster stars N, the number of simulations $N_{\rm sim}$ performed for a given model, the initial concentration W_0 of the King model, the upper mass limit of the IMF, the initial cluster mass, and the half-mass radius. Also shown are the final half-mass radius and the BH masses at the start and the end of the runs. The final column gives the (average) number of tidal disruptions.

3. RESULTS

3.1. *Cluster Expansion*

Figure 1 depicts the evolution of Lagrangian radii for the first four clusters of Table 1. All clusters expand, since the mass loss of individual stars due to stellar evolution decreases the potential energy of the clusters and two-body processes in the cusp around the BH exchange energy between the stars. As a result, the innermost stars are pushed to more negative energies until they are tidally disrupted by the IMBH, while the rest of the cluster stars gain energy and the cluster expands. This behavior is similar to that seen in the single-mass runs of Paper I (Fig. 5).

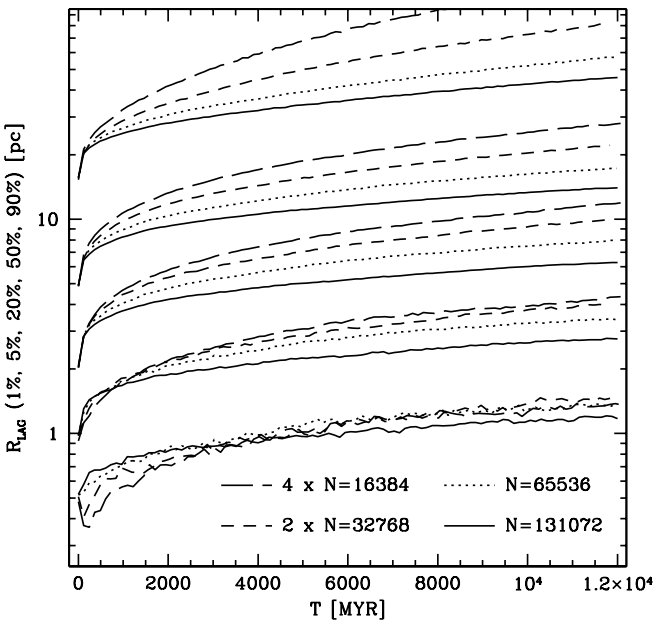

FIG. 1.—Lagrangian radii as a function of time for the first four cluster simulations with particle numbers $16,384 \le N \le 131,072$. All clusters expand as a result of energy generation in the cusp around the BH and initially also because of stellar evolutional mass loss, which decreases the binding energy of the cluster. Since two-body relaxation drives the expansion, high-N models expand less than low-N ones.

For all clusters the expansion is strongest in the initial phase, since the cluster radii and therefore the two-body relaxation time is smallest in the beginning. In addition, the mass loss of stars due to stellar evolution is strongest within the first gigayear. The expansion is smaller for high-N clusters owing to their longer relaxation times. Table 1 shows that for a given mass of the central BH, the final half-mass radius depends only on the number of cluster stars and is nearly independent of the cluster composition and initial half-mass radius. For the $N = 16$K clusters, for example, the final half-mass radius changes by less than 10% if the initial half-mass radius is reduced by a factor of 6. The final radius also does not depend much on the initial IMF or the initial concentration of the King model.

The two-body relaxation time of a cluster with mass $M_{\rm Cl}$ and radius r_h is given by (Spitzer 1987)

$$T_{\rm RH} \sim \frac{\sqrt{M_{\rm Cl}}\, r_h^{3/2}}{\langle m \rangle \sqrt{G}\ln(\gamma N)} \qquad (2)$$

for a cluster with stars of average mass m. If the cluster expansion is caused by two-body relaxation, half-mass radii of clusters with masses $M_{\rm Cl}$ should satisfy a relation $r_h \sim M_{\rm Cl}^{-1/3}$ after a long enough time has passed, since the half-mass relaxation time is the same for all clusters in this case so they expand with the same rate. The final half-mass radii of the clusters in Table 1 are in good agreement with such a scaling law.

Figure 2 compares the projected half-light radii of the clusters in Figure 1 with the projected half-light radii of Galactic globular clusters. The results of the N-body simulations are well fitted by an $r_{h,p} \sim M_{\rm Cl}^{-1/3}$ law (*solid line*), so projected half-mass and half-light radii follow the same relation as the three-dimensional ones. Projected half-light radii of Galactic globular clusters are taken from Harris (1996). Masses for globular clusters were calculated from their absolute V magnitudes, assuming a mass-to-light ratio of $m/L_V = 2.0$. Most globular clusters have projected half-light radii that are smaller than those predicted by an extrapolation of our runs.

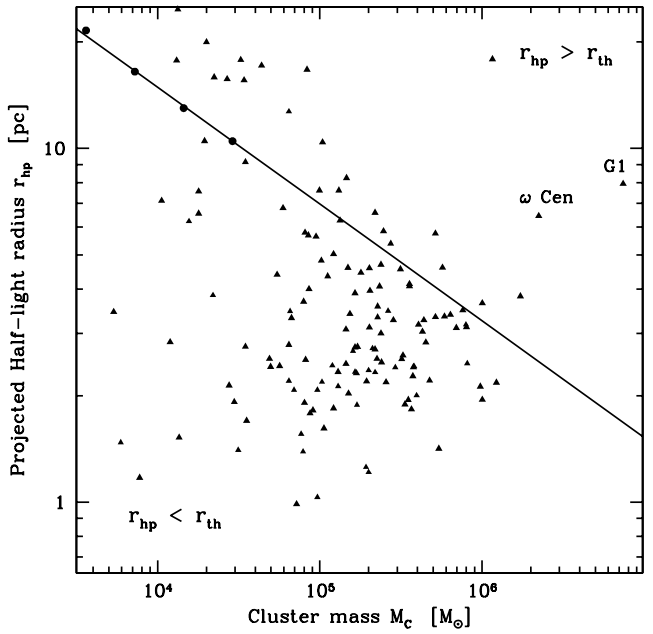

FIG. 2.—Projected half-light radii of globular clusters $r_{h,p}$ against their mass (*triangles*). Projected half-light radii of the clusters in the *N*-body simulation are marked by filled circles. They follow a relation $r_{h,p} \sim M_{\rm Cl}^{1/3}$ (*solid line*), in agreement with the idea that two-body relaxation drives the cluster expansion. The expansion due to an IMBH is strong enough that clusters with IMBHs can end up among the least concentrated clusters.

Rasio et al. (2004) and Portegies Zwart et al. (2004) have shown that core-collapse times of less than a megayear are necessary to form an IMBH in the center of a star cluster by runaway collision of main-sequence stars. For high-*N* clusters, this corresponds to central densities of $\rho_c = 10^6\ M_\odot\ {\rm pc}^{-3}$ or higher. Most other processes that have been proposed as formation mechanisms for IMBHs also require high-density environments. Such densities are among the highest found in globular clusters (see Table 2 of Pryor & Meylan 1993). Figures 1 and 2 show that even if clusters with massive BHs start with very high densities, the subsequent cluster expansion increases their radii by such an amount that they can end up among the least dense clusters. Thus, the low density of present-day globular clusters does not rule out the formation of IMBH, since they might have been much more compact when they were born.

The fact that most clusters have half-light radii below our prediction does not speak against the presence of IMBHs in these clusters, since, while our clusters were isolated, Galactic globular clusters are surrounded by a tidal field, which limits their growth. Tidally limited clusters that lie below our predicted line might therefore still contain IMBHs.

The half-mass radius of G1, the most massive globular cluster in M31, is $r_h = 8$ pc (Baumgardt et al. 2003b). If G1 started much more concentrated and its current size is due to an expansion similar to the one seen in our runs, the mass of the central IMBH must be larger than 1000 $M_\odot$, since the half-mass radius of G1 is much higher than predicted by our runs. The same is true for ω Cen, the most massive Galactic globular cluster.

3.2. *Density Profile*

In Paper I it was shown that the density profile of a single-mass cluster follows a power-law profile $\rho \sim r^{-\alpha}$ inside the influence radius of the BH with slope $\alpha = 1.75$, in agreement with results from Fokker-Planck and Monte Carlo simulations. It was also shown that the sphere of influence of the BH is limited by two conditions. For low-mass BHs, clusters have a near constant-density core outside the sphere of influence of the BH and the central cusp extends only up to a radius r_i at which the velocity dispersion in the core becomes comparable to the circular velocity of stars around the BH. The following relation was found to give a good estimate for r_i:

$$r_i = \frac{GM_{\rm BH}}{2\langle v_c^2 \rangle}, \tag{3}$$

where v_c is the core velocity dispersion. For BHs that contain more than a few percent of the cluster mass, a second condition for r_i was found to be that the mass in stars inside r_i must be smaller than the mass of the central BH, since otherwise the self-gravity of stars becomes important and changes the density law.

Figure 3 depicts the final density profile of the first four clusters after 12 Gyr. Shown is the three-dimensional mass density of all stars. In order to calculate the density profile, we have superposed between 5 (128K) and 20 (16K) snapshots centered at $T = 12$ Gyr, creating roughly the same statistical uncertainty for all models. All snapshots were centered on the position of the IMBH. We then fitted the combined density profile inside the influence radius of the BH with a power-law density profile. It can be seen that we obtain a power-law profile inside r_i with slope around $\alpha = 1.55$. There is no visible dependence on the particle number. It is shown in § 3.3, where the mass segregation in the clusters is discussed, that the most massive stars in our clusters still follow an $\alpha = 1.75$ power law but that they are not numerous enough to dominate the central region, which is the reason for the flatter overall slope seen in our runs.

For $N = 16$K, the BH contains more than 10% of the total cluster mass at $T = 12$ Gyr and it dominates the density profile throughout the core. For clusters with particle numbers more realistic for globular clusters, the central BH contains an increasingly smaller fraction of the total cluster mass, so the velocity criterion limits the influence of the BH. In this case, the central cusp contains only a fraction of the mass of the central BH; for $N = 128$K, for example, only ~10%, i.e., 100 $M_\odot$. Since a considerable fraction of these stars would not be easily visible to an observer because they are compact remnants and therefore too faint, the direct observation of this cusp for globular clusters with $M_{\rm BH} < 1000\ M_\odot$ IMBHs is nearly impossible because of statistical uncertainties.

The upper panel of Figure 4 depicts the projected distribution of bright stars for the cluster with $N = 128$K stars. We define bright stars to be all stars with masses larger than 90% of the mass of turnoff stars that are still main-sequence stars or giants at $T = 12$ Gyr. Their density distribution should be representative of the distribution of light in the cluster. The projected density distribution of bright stars does not show a central rise and can instead be fitted by a model with a constant density core according to

$$\rho = \frac{\rho_0}{(1 + r/a)^5}, \tag{4}$$

where ρ_0 and a are constants. A cluster with a massive central BH would therefore appear as a standard King profile cluster to an observer, making it virtually indistinguishable from a

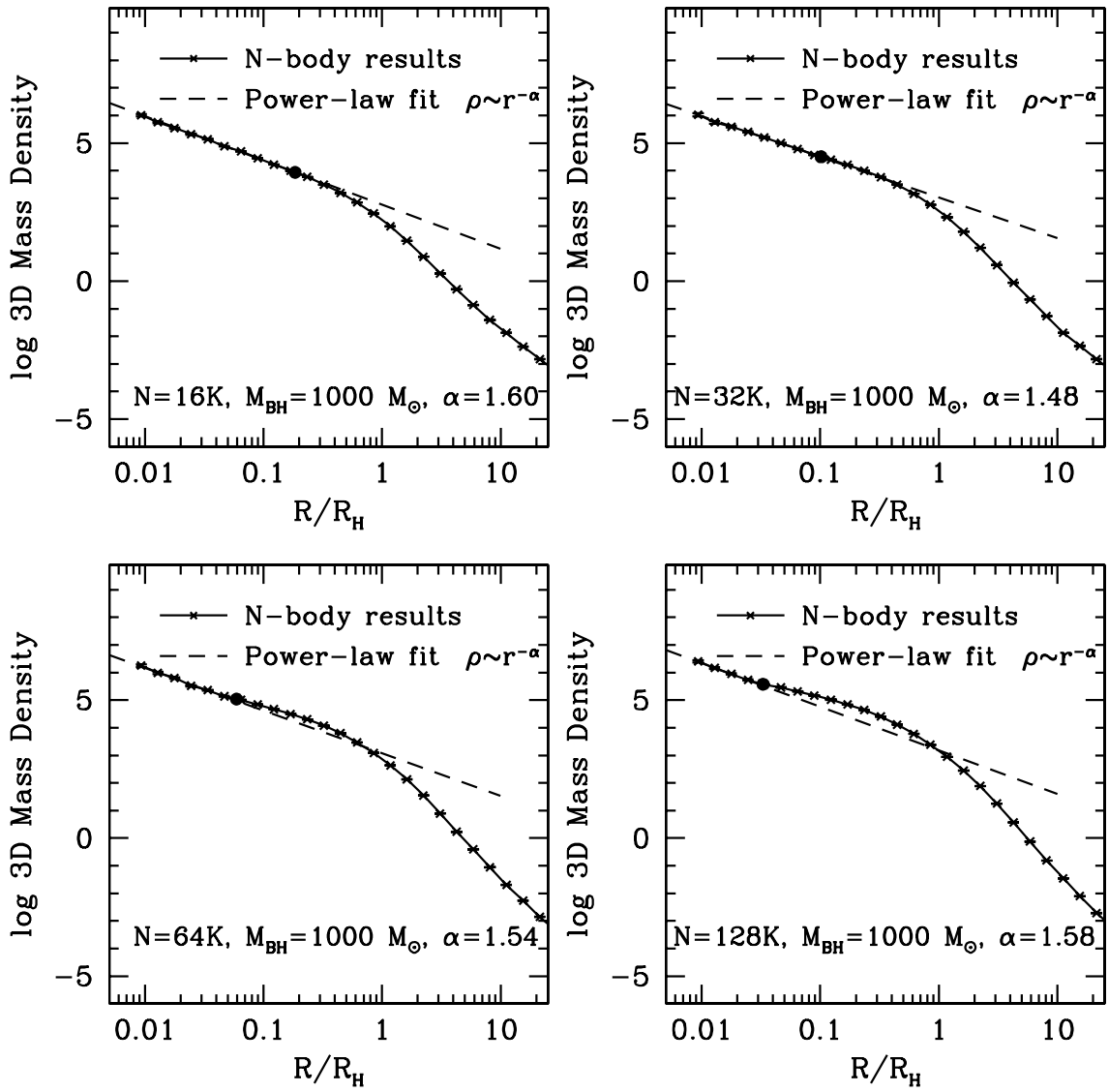

FIG. 3.—Three-dimensional mass density profile after $T = 12$ Gyr for four cluster simulations starting with particle numbers $16,384 \leq N \leq 131,072$. Solid lines mark the *N*-body results and dashed lines mark a single power-law fit to the density profiles inside the radius of influence of the BH (shown by a solid circle). For all models we obtain slopes near $\alpha = 1.55$ for the central stellar cusp.

star cluster before core collapse. Core-collapse clusters have central density profiles that can be fitted by power laws with slopes of $\alpha \approx 0.7$ (Lugger et al. 1995), which is in contradiction with this profile. Since the central relaxation times of core-collapse clusters are much smaller than a Hubble time, any cusp profile would have been transformed to a constant density core if an IMBH were present in any of these clusters (see Fig. 5). The presence of IMBHs in core-collapse clusters is therefore ruled out unless their composition is radically different from our clusters.

The lower panel of Figure 4 shows the measured velocity dispersions and those inferred from the mass distribution of stars. The inferred velocity dispersions were calculated from the Jeans equation (Binney & Tremaine 1987, eq. [4.54]) and different mass distributions under the assumption that the velocity distribution is isotropic (i.e., $\beta = 0$). The velocities calculated from the mass distribution of the cluster stars alone give a good fit at radii $r/r_h > 0.2$, where the mass in stars is dominating (except at the largest radii, where the velocity distribution becomes radially anisotropic). At radii $r/r_h < 0.2$, the contribution of the BH becomes important. At a radius $r/r_h = 0.01$, the velocity dispersion is already twice as high as the one due to the stars alone. For a globular cluster at a distance of a few kiloparsecs, such a radius corresponds to central distances of $1''$ or $2''$. On the order of 20 stars would have to be observed to detect the central rise at this radius with a 95% confidence limit. This seems possible both for radial velocity (Gerssen et al. 2002) or proper motion studies (McNamara et al. 2003) with *HST*. For a nearby globular cluster, the detection of a massive central BH through kinematical studies is therefore possible. Similarly, Drukier & Bailyn (2003) concluded that the IMBH can be found by studying the tail of the velocity distribution through proper motions.

Figure 5 shows the projected density distribution of stars for the $N = 128$K cluster at four different times. In the beginning, the cluster has a constant-density core due to the initial King model. As the cluster evolves, a central cusp forms around the BH. This cusp is visible in projection already after $T = 200$ Myr and is fully developed around $T = 1$ Gyr. Since both

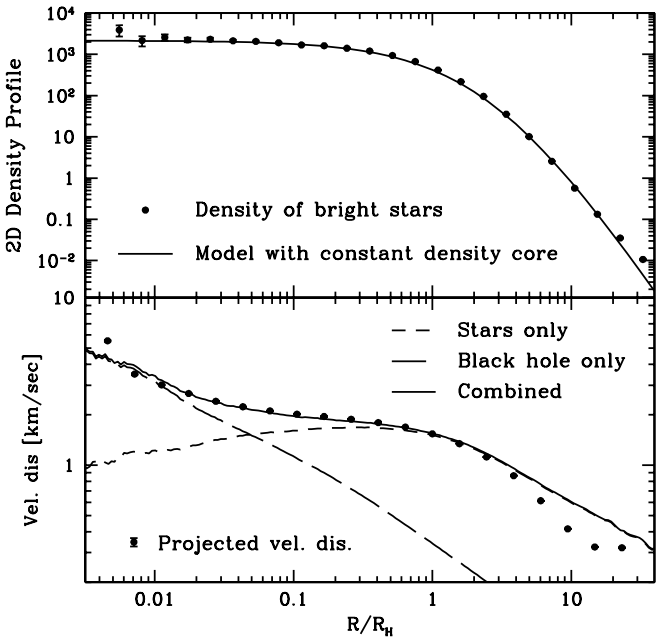

FIG. 4.—Projected density profile of bright stars (*top*) and the projected velocity dispersion of the cluster simulation starting with $N = 131,072$ stars. The projected distribution of bright stars has a constant density core, similar to that seen in most globular clusters. Observations of the velocity dispersion could reveal the BH if a sufficiently large number of stars at radii $r/r_h < 0.01$ can be observed (*bottom*).

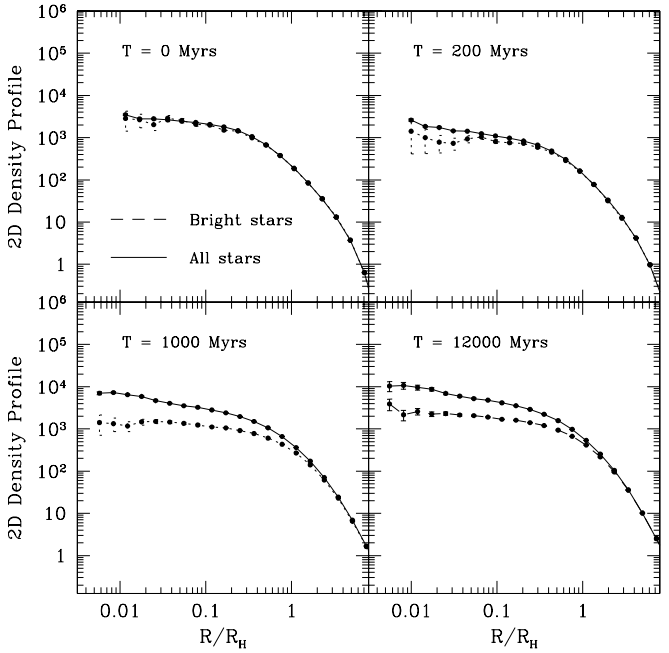

FIG. 5.—Projected density distributions of stars for four different times for the cluster with $N = 131,072$ stars. The densities of bright stars and of all stars are shifted to match each other at $r = 10r_h$. The density distribution of all stars develops a cusp profile after a few 100 Myr. Bright stars show a constant-density core throughout the evolution.

times are much smaller than a Hubble time, globular clusters that formed an IMBH early on in their evolution have reached an equilibrium profile in their center. Throughout the evolution, the distribution of bright stars displays a constant-density core, since mass segregation leads to an enhancement of high-mass compact remnants in the center. Except for the very first phases after IMBH formation, in which the density distribution might differ from the King profiles with which we started, clusters with massive BHs should exhibit constant-density cores in their light profile.

3.3. *Mass Segregation*

Because of relaxation, massive stars sink into the center of a star cluster in order to achieve energy equipartition between stars of different masses (Spitzer 1969). Baumgardt & Makino (2003) and Gürkan et al. (2004) showed that mass segregation of high-mass stars proceeds on the same timescale as the evolution of the clusters toward core collapse. Baumgardt & Makino (2003) also found that by the time a globular cluster goes into core collapse, the majority of stars in the core are compact remnants.

Figure 6 shows the average mass of stars in the core (defined to contain the innermost 3% of the cluster mass) and the average mass of all cluster stars for the first four clusters of Table 1. The average mass of all cluster stars (*dashed lines*) drops because of stellar evolution, which is most effective within the first gigayear. For low-N models the core mass rises initially, since the relaxation time is short enough to allow heavy main-sequence stars to spiral into the core. For higher N models, the relaxation time is larger than the stellar evolution time, and stars with masses $M > 5\ M_\odot$ turn into compact remnants and lose a large fraction of their mass before reaching the core.

For $N = 64$K stars, we also performed a comparison run that started from a King $W_0 = 7.0$ model with the same IMF as the other clusters, but did not contain an IMBH (*dotted lines in lower left panel*). The average mass of stars in the core for the $N = 64$K cluster without a BH rises as the cluster evolves toward core collapse (reached at $T = 10.5$ Gyr). Because of the choice of IMF, there are only a few BHs present in this model, so by the time core collapse has been reached the average mass of stars in the core is roughly equal to the mass of the most heavy white dwarfs and neutron stars. This mass stays nearly constant in the postcollapse phase.

In contrast, in clusters with IMBHs the average mass of stars in the core reaches $\langle m \rangle = 0.6\ M_\odot$ after 2–3 Gyr and stays more or less constant afterward. There is no dependence of the average core mass on the particle number and no time evolution. This implies that our clusters have reached an equilibrium state in which heavy stars sink into the cusp because of mass segregation and are expelled equally rapidly from the cluster center by a balancing process. The most likely driving force for this balancing process is close encounters between stars in the cusp. In Paper I it was shown that close encounters are efficient in removing stars from the cusp, since the average velocities are high, so stars scattered out of the cusp leave the cluster completely or are scattered into the halo and take a long time to reach the core again. The average stellar mass in the core is similar for star clusters with IMBHs and precollapse star clusters without IMBHs, making a distinction between both types of clusters through star counts difficult.

Figure 7 shows the density distribution of stars of different mass groups for the cluster with $N = 131,072$ stars. Within the uncertainties, density distributions of different mass groups can be fitted by power laws. The exponents α decrease from the high-mass stars to the lighter stars, since mass segregation enhances the density of high-mass stars in the center. If we exclude the few stellar-mass BHs, the most massive stars are massive white dwarfs, which have masses $m < 1.2\ M_\odot$.

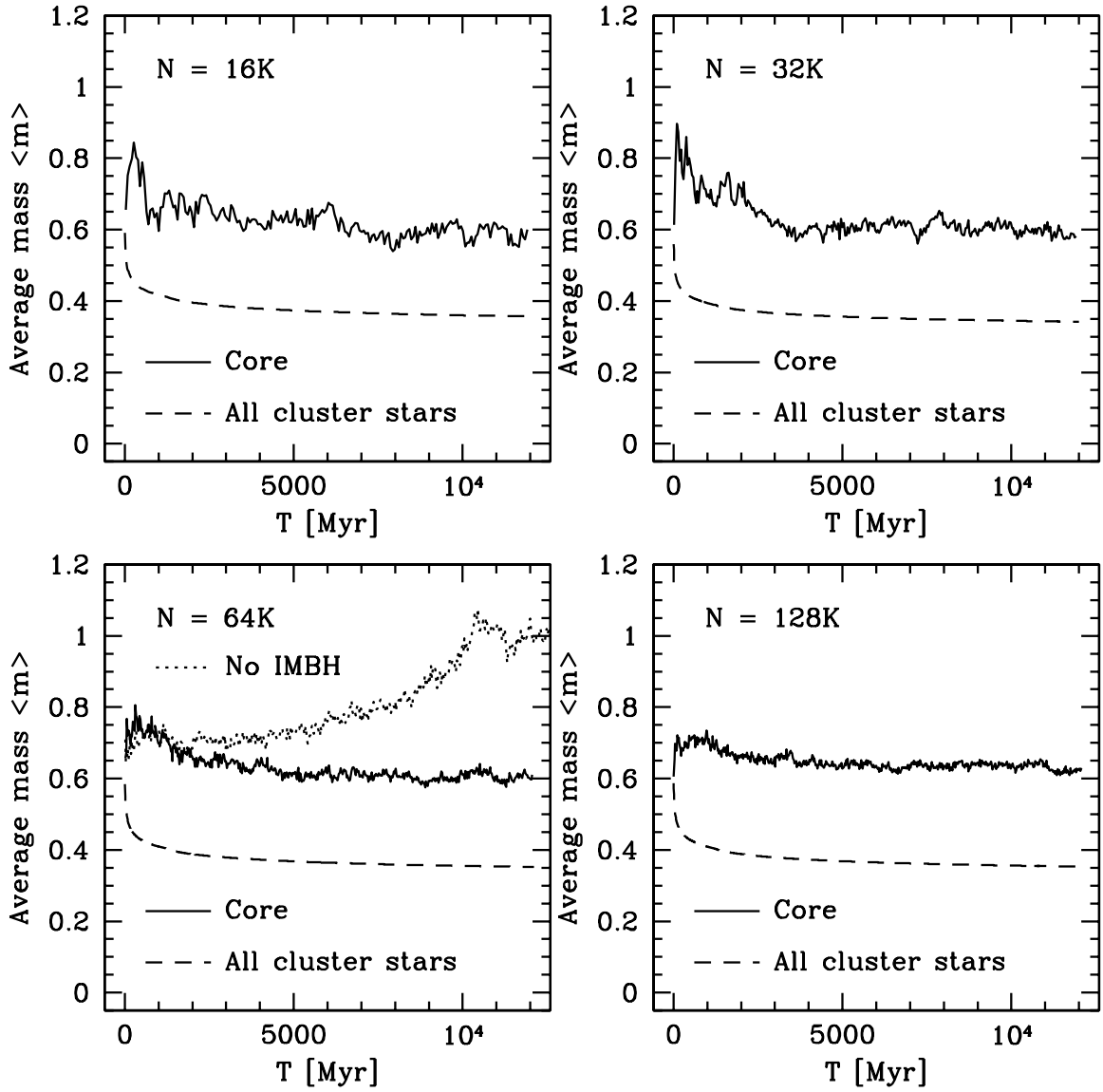

FIG. 6.—Average mass of stars in cluster simulations with different particle numbers. In a cluster without an IMBH (*dotted line*, $N = 64$K) the average mass in the core increases until it reaches a maximum at core-collapse time ($T = 10.5$ Gyr). In contrast, the average core mass for clusters with IMBHs stays nearly constant throughout the evolution at $\langle m \rangle = 0.6$, independent of N.

Figure 7 shows that their density distribution follows a power law with exponent $\alpha = 1.68$. For the $N = 32$K and 64K clusters we obtain similar exponents of $\alpha = 1.80$ and 1.82 for the high-mass stars. Given the error with which α can be determined, all values are probably compatible with an exponent of $\alpha = 1.75$. Bahcall & Wolf (1977) showed that in a two-component system, stars of the heavier mass group follow a power-law distribution with $\alpha = 1.75$ in the cusp around the BH. Our simulations are an extension of their work to multicomponent systems. Here again the heaviest stars follow an $\alpha = 1.75$ law. Since the mass in the heaviest mass group is only a small fraction of the total cusp mass, the actual density distribution of the cusp is flatter than an $\alpha = 1.75$ power law. The slope α for stars of average mass m can be approximated by

$$\alpha_{(m)} = 0.75 + m/1.1. \quad (5)$$

We find that this density law is a good fit to all runs. Tremaine et al. (1994) showed that the slope α of the stellar density distribution around a BH has to fulfill the condition $\alpha > 1/2$ if the velocity distribution is isotropic, since otherwise the average velocity of stars at a given radius r in the cusp would become larger than the escape velocity at this radius. The density profile of the lowest mass stars is indeed above this limit, even if the argument is not a strict argument for our case since Tremaine et al. considered only the escape from the potential of the BH, while here the main cluster mass is in the form of stars.

3.4. *Tidal Disruption of Stars*

Figure 8 shows the relative fraction of disrupted stars in the simulations for clusters with particle numbers between $16,384 \leq N \leq 131,072$. The stars in our simulations fall roughly into four different categories: main-sequence stars, giants, white dwarfs, and neutron stars and BHs. Mostly main-sequence stars are disrupted, since they are abundant and have relatively large radii. Giants also contribute significantly, despite their low numbers. Our simulations show that most

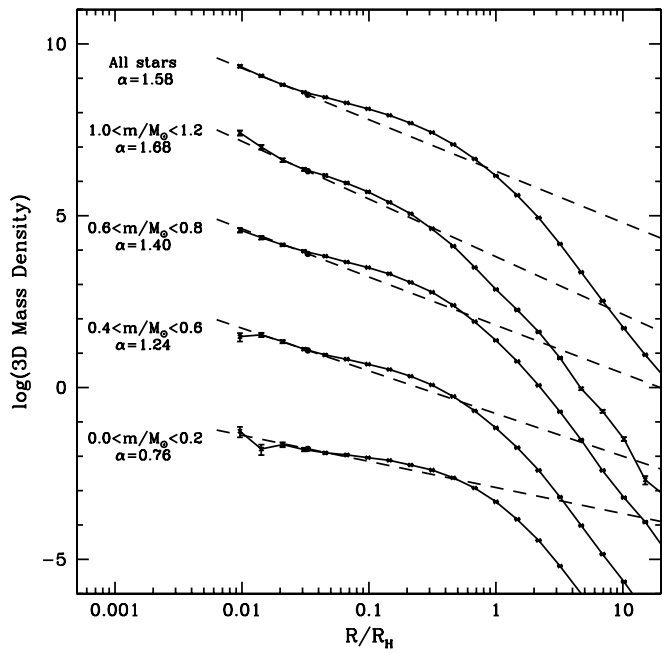

FIG. 7.—Density of different mass groups as a function of radius for the $N = 128$K star cluster at $T = 12$ Gyr. Stars in the most massive group follow a distribution that drops as $\alpha \approx 1.75$ in the cusp around the BH. For lower mass stars, the cusp profile becomes increasingly flatter. The overall mass density drops with an average value near $\alpha = 1.55$, since too few high-mass stars are in the cusp to dominate the profile.

giants are disrupted within the first Gyr. There are no significant differences in the disruption rates between individual runs. Taking the mean over all simulations, we find that $72\% \pm 7\%$ of all disrupted stars are main-sequence stars, $19\% \pm 3\%$ are giants, and $9\% \pm 2\%$ are white dwarfs. During our simulations no neutron stars or BHs merged with the central IMBH. However, the merging rate of neutron stars and BHs could be underestimated, since our simulations did not include gravitational radiation, the effects of which are discussed in § 3.6.

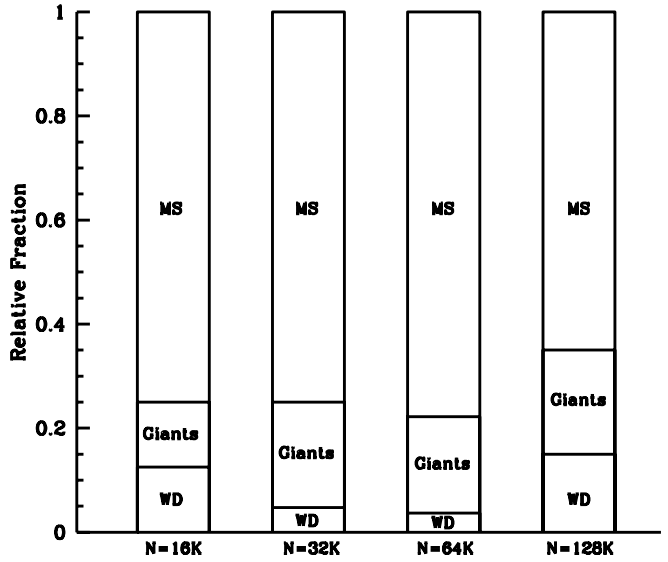

FIG. 8.—Relative fraction of disrupted stars for cluster simulations with different particle numbers. IMBHs in globular clusters preferentially disrupt main-sequence stars and giants, with white dwarfs accounting for only 10% of all disrupted stars. The number of disrupted neutron stars is negligibly small.

Using the loss cone theory developed by Frank & Rees (1976), one can show with an argument similar to that in Paper I that the rate at which stars are disrupted by a central BH is proportional to

$$D \sim \sqrt{G}\left(\frac{r_T^{9-4\alpha} n_0^7 m^{4\alpha-2}}{M_{\rm BH}^{5\alpha-6}}\right)^{1/(8-2\alpha)}, \qquad (6)$$

where r_T is the tidal radius of stars, m is their average mass, and n_0 is a constant that describes the number density of stars in the central cusp around the BH, $n(r) = n_0 r^{-\alpha}$. With the help of equation (1), we can rewrite this as

$$D = k_D \sqrt{G}\left[\frac{R_*^{9-4\alpha} n_0^7 m^{(16/3)\alpha-5}}{M_{\rm BH}^{19/3\alpha-9}}\right]^{1/(8-2\alpha)}. \qquad (7)$$

In globular clusters, the radii and masses of stars differ, so disruption rates have to be calculated separately for each stellar type.

By comparing the actual number of disruptions and the estimated number from equation (7), we can determine the coefficient k_D. In order to do this, we calculated n_0 for all the times data was stored from the stars inside the cusp and integrated equation (7) over time to obtain the expected number of disruptions for each run and each stellar species. In order to calculate n_0, we assumed $\alpha = 1.55$ for main-sequence stars and giants and $\alpha = 1.75$ for compact remnants. The disruption constants k_D and the amount by which different stellar species should contribute can be found in Table 2. Most simulations are compatible with $k_D = 65$, which was also found in the single-mass runs of Paper I. In agreement with the simulations, we expect most disrupted stars to be main-sequence stars. Giants and white dwarfs should account for ~25% of all disruptions and the rate at which neutron stars are disrupted is negligible, in agreement with the fact that no such disruptions were observed in our N-body runs. The relative fraction of disrupted giants and white dwarfs agrees very well with the results of our runs. Most stars are disrupted within the first 2 Gyr, when the clusters are compact and the densities around the IMBHs are high.

In order to apply our disruption rates to real globular clusters, for which the density n_0 of the central cusp is unknown, we have to connect n_0 to the core density n_c. We assume that the cusp density rises with $\alpha = 1.55$ and that the cusp goes over into a constant density core with density n_c at

TABLE 2
MERGER RATES OF DIFFERENT STELLAR SPECIES

N	k_D	$f_{\rm MS}$	$f_{\rm Giant}$	$f_{\rm WD}$	$f_{\rm NS}$
16384	65 ± 11	0.76	0.15	0.08	1×10^{-8}
32768	83 ± 18	0.76	0.15	0.08	5×10^{-9}
65536	59 ± 12	0.74	0.17	0.09	2×10^{-9}
131072	46 ± 7	0.73	0.20	0.07	2×10^{-9}
32768	58 ± 41	0.88	0.04	0.08	3×10^{-5}
65536	63 ± 27	0.84	0.04	0.11	5×10^{-6}
131072	86 ± 23	0.83	0.09	0.08	3×10^{-6}

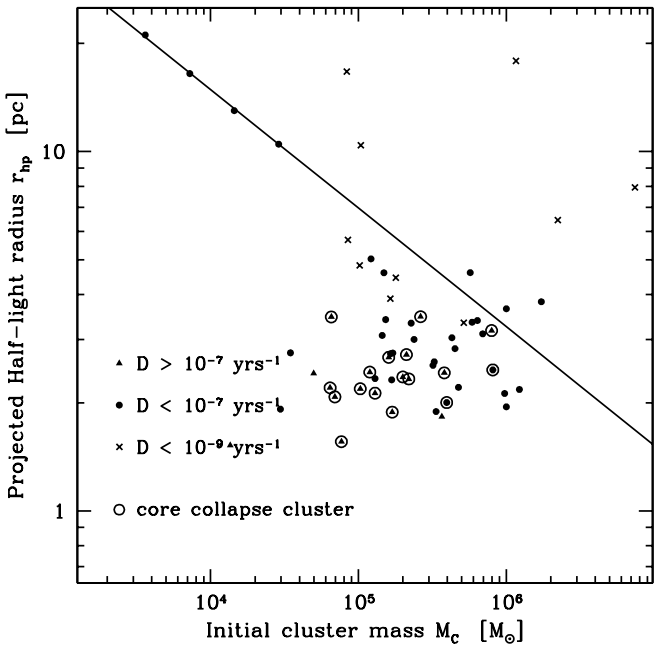

FIG. 9.—Disruption rates D for globular clusters from the list of Pryor & Meylan (1993) for which central velocity dispersions and densities are available. Core-collapse clusters have high disruption rates, but their morphology shows that they cannot contain IMBHs. All clusters that follow the mass-radius relation predicted by our runs have only small disruption rates, making it unlikely that the IMBHs would be visible as X-ray sources.

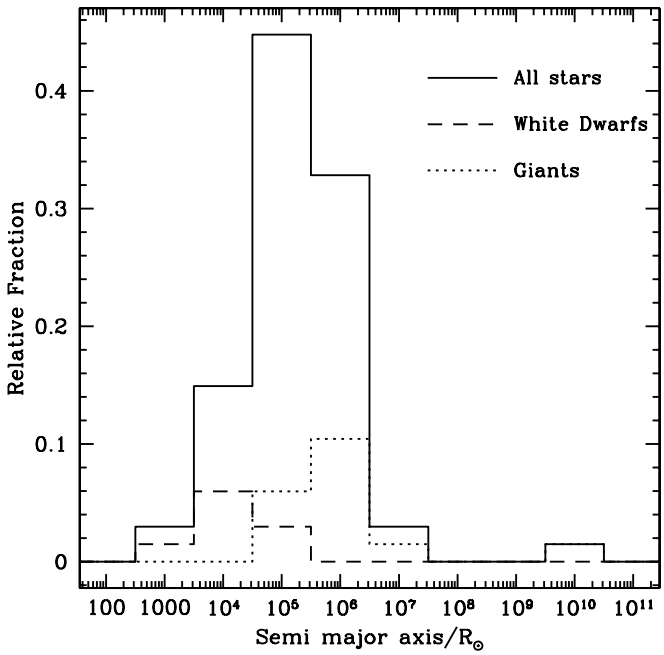

FIG. 10.—Semimajor axis distribution, a, of stars disrupted by the BH in the $N = 65,536$ and 131,072 cluster simulations. Most stars move on highly eccentric orbits with $a \gg r_T$ when they are disrupted by the BH. Disrupted white dwarfs move on orbits with semimajor axes that are about a factor of 10 smaller than those of main-sequence stars.

the influence radius of the BH, given by equation (3). With this, the disruption rate becomes

$$D = \frac{1.13}{100\ \mathrm{Myr}} \left(\frac{R_*}{R_\odot}\right)^{3/5} \left(\frac{m}{M_\odot}\right)^{3/5} \left(\frac{M_{\mathrm{BH}}}{1000\ M_\odot}\right)^{2} \times \left(\frac{n_c}{10^5\ \mathrm{pc}^{-3}}\right)^{7/5} \left(\frac{v_c}{10\ \mathrm{km\ s}^{-1}}\right)^{-21/5}. \quad (8)$$

Using this formula and the velocities and central densities of globular clusters given in Pryor & Meylan (1993), we can calculate the disruption rates D for globular clusters. We assume an average stellar mass in the core of $m = 0.6\ M_\odot$ and a stellar radius $R_* = 0.7\ R_\odot$. The results are shown in Figure 9. Core-collapse clusters have D values of up to several times 10^{-5} yr^{-1} because of their high central densities. However, their morphology rules out IMBHs, as was shown in § 3.2. Among the non–core-collapse clusters, three clusters (NGC 1851, NGC 4147, and NGC 6336) have $D > 10^{-7}$ yr^{-1}, so a 1000 $M_\odot$ IMBH could double its mass within a Hubble time. The disruption rate is also high enough that X-ray flares from material falling onto the central BH could be observable, depending how long it takes for the material to be swallowed by the central BH. These clusters are, however, more concentrated than we would expect if they contain IMBHs. Clusters that have sizes that agree with our predicted ones have fairly small disruption rates of $D < 10^{-9}$ yr^{-1}, i.e., less than one star per gigayear. The BHs in such clusters would therefore remain inactive for most of the time. If we start from a 50 $M_\odot$ seed BH, the disruption rates would drop to less than 2.5×10^{-10} yr^{-1} according to equation (8), even for the most promising clusters. Therefore, the growth of an IMBH from a BH produced by normal stellar evolution through the tidal disruption of stars is impossible, unless the cluster is initially significantly more concentrated than any cluster we see today.

Figure 10 shows the semimajor axis distribution of stars disrupted by the IMBH on their last orbit prior to disruption. Shown is the combined distribution for the $N = 64$K and $N = 128$K clusters that are closest to real globular clusters. All stars have semimajor axes a that are far larger than their tidal radii, similar to the situation found for single-mass clusters in Paper I. The most important mechanism for the disruption of stars is therefore again drift in angular momentum space. Material from disrupted stars will first move in a highly eccentric ring around the IMBH. The ring shrinks because of viscous heating until the gas from the disrupted star forms an accretion disc around the IMBH. Since there are other stars moving inside the initial orbit of the disrupted star that can scatter away material or swallow it, the fraction of material that is finally swallowed by the IMBH is rather uncertain.

Because of their smaller radii, disrupted white dwarfs also come from smaller distances. According to the theory developed in Paper I for single-mass clusters, their average semimajor axis should be smaller by about $(R_{\mathrm{MS}}/R_{\mathrm{WD}})^{4/9} \approx 10$, which is in good agreement with the results in our simulations. Similarly, giants come from larger distances on average.

3.5. *Clusters with High-Mass Black Holes*

We now discuss the evolution of clusters that started with a mass function extending up to 100 $M_\odot$. These clusters contained a significant number of stellar-mass BHs. The highest mass BHs formed had ~45 $M_\odot$ and we assumed a 100% BH retention rate, so the true fraction of BHs in globular clusters will probably be somewhere between the situation in these runs and the previous ones. Cluster radii were chosen such that the relaxation time was the same in all runs and equal to the

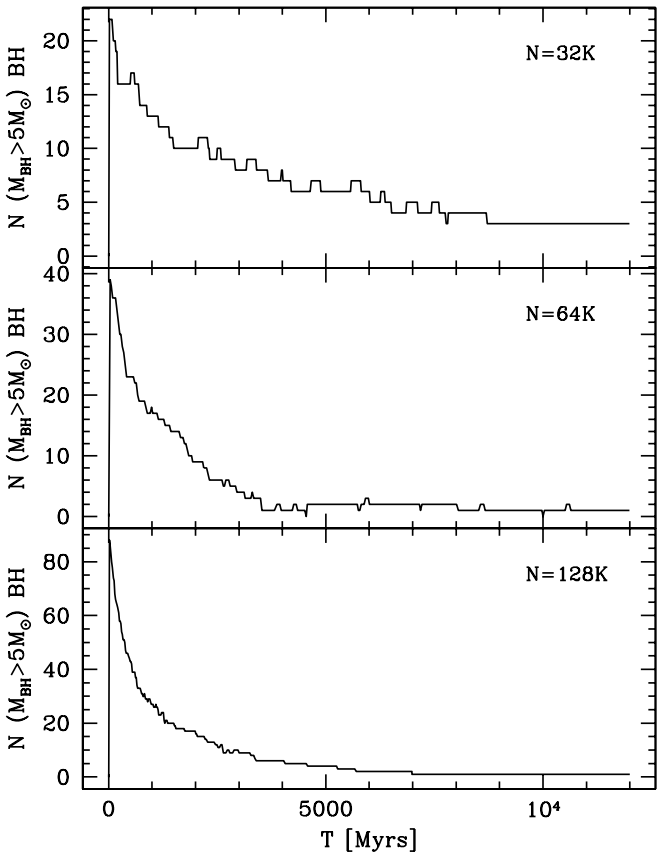

FIG. 11.—Number of bound BHs with masses $M_{\rm BH} > 5\ M_\odot$ in the runs with a high upper mass limit. The number decreases because of close encounters between the BHs in the central cusp around the IMBH. After several gigayears, only one high-mass BH remains in most cases. This is the object most deeply bound to the central IMBH and has absorbed the energy from the encounters that ejected the other BHs.

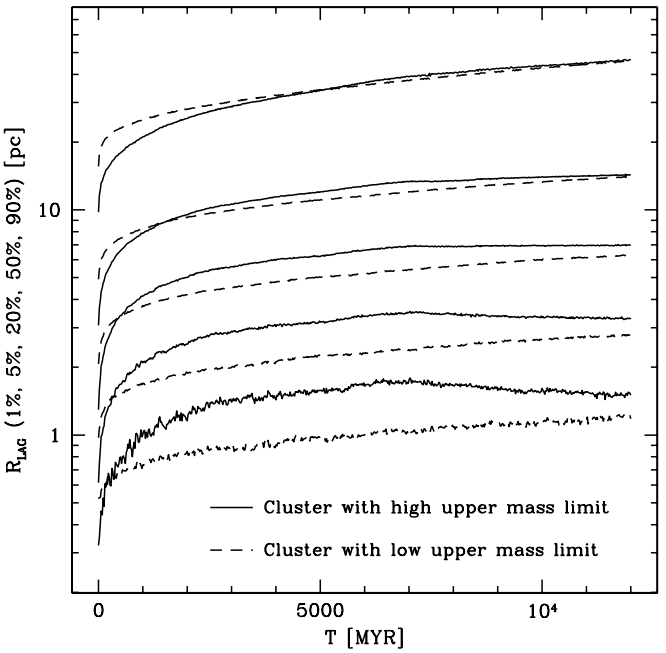

FIG. 12.—Evolution of Lagrangian radii for two $N = 128$K clusters, one having an IMF extending up to $m = 100\ M_\odot$ and many high-mass BHs and one with a lower high-mass cutoff of 30 $M_\odot$. The cluster with many BHs expands more strongly initially because of the efficient heating of the BHs. Nevertheless, the final radii are almost the same for both clusters.

relaxation time of a dense globular cluster with $M_{\rm Cl} = 10^6\ M_\odot$ and $r_h = 1$ pc.

Massive BHs are initially produced throughout the clusters and sink toward the centers because of mass segregation. Figure 11 shows the number of BHs bound to the clusters as a function of time. The number of heavy stellar-mass BHs drops, since close encounters between the BHs in the cusp around the IMBH remove them from the cluster. Since the velocity in the cusp is relatively high, such encounters mostly lead to the ejection of one of the BHs. For the $N = 64$K and 128K clusters, only one massive BH remains in the cluster after several gigayears have passed. For the $N = 32$K cluster, three remained; however, two of them were in orbits far away from the cluster center and would have been lost from the cluster if the cluster had been surrounded by a galactic tidal field. In all three clusters, the BH that remains is the star most closely bound to the central IMBH (see Fig. 14) and is among the most heavy BHs produced. This resembles the situation in our runs with the lower upper mass limit. As the relaxation time in our runs is similar to that of dense, massive globular clusters, we expect that clusters with IMBHs also contain only a few other massive BHs, and the star most closely bound to the IMBH should be another BH.

A look at the Lagrangian radii (Fig. 12) shows that the overall expansion is slightly different from the previous case. Clusters expand more rapidly in the beginning, when they still contain many high-mass BHs. These are very effective in scattering low-mass stars to less bound orbits while sinking into the cluster center. The innermost radii of the cluster with $N = 128$K stars and a high upper mass limit decrease slightly after $T = 7000$ Myr. This is due to the loss of the second-nearest star to the IMBH through a close encounter with the innermost star (see Fig. 14). The second-nearest star was an efficient heat source, since it was a 15 $M_\odot$ BH that moved in a relatively wide orbit around the IMBH, bringing it into frequent encounters with field stars. After this BH is lost, the innermost radii shrink to adjust themselves and the energy generation rate in the center to the size of the half-mass radius. The final radii of clusters with high-mass BHs are within 10% of the radii of runs with the same N but a lower upper mass limit (see Table 1). The initial radii were different for $N \geq$ 64K stars, but it was shown in § 3.1 that the initial radii do not influence the final radii much. We therefore conclude that the IMF does not significantly affect the final radius either.

Figure 13 depicts the density distribution of the $N = 128$K cluster after 12 Gyr. As in the case of a cluster starting with only few BHs, high-mass stars follow a steeper density distribution and are enriched in the cluster center. The overall slopes for stars of the same mass are very similar to the low upper mass limit case, since most high-mass BHs have been lost from the cluster by this time, so the overall mass function of stars is nearly identical. Again, when viewed in projection this cluster would appear as a cluster with a constant density core. The average mass of stars in the core is the same as in the previous case, $\langle m \rangle = 0.6\ M_\odot$, independent of N.

The merger rates of different stars for clusters with a high upper mass limit can be found in Table 2. Compared to the lower mass limit case, the fraction of neutron star and BH disruptions is increased by a factor of 100 because of their higher density around the IMBH in the initial phases. The overall fraction is, however, still negligible. The merger rate for giants decreased since the high-mass stellar-mass BHs

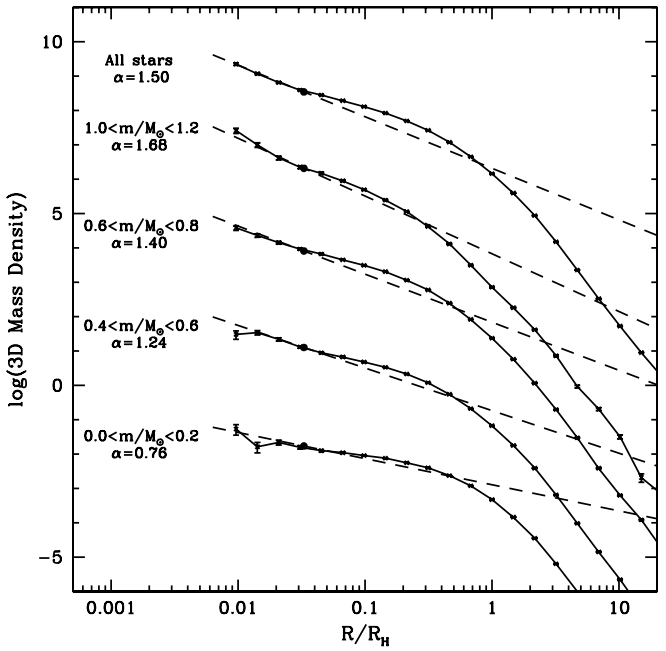

FIG. 13.—Density of different mass groups as a function of radius for the $N = 128$K star cluster with a high upper mass cutoff at $T = 12$ Gyr. The power-law slopes are similar to that of the cluster with a low upper mass limit. High-mass stars are again enriched in the cluster center.

prevent giants from accumulating near the IMBH in the initial phases. The effect is less visible for the $N = 128$K clusters, in which the disruption rate is already quite similar to the run with the low upper mass limit. The constant for the overall disruption rate k_D stayed more or less the same, so our previous conclusions still hold if we change the mass function. This is despite the fact that the IMBH is forced to move with a larger amplitude, since the star most closely bound to the IMBH is now 20 times more massive. The movement of the central BH therefore does not have much effect on the merging rate.

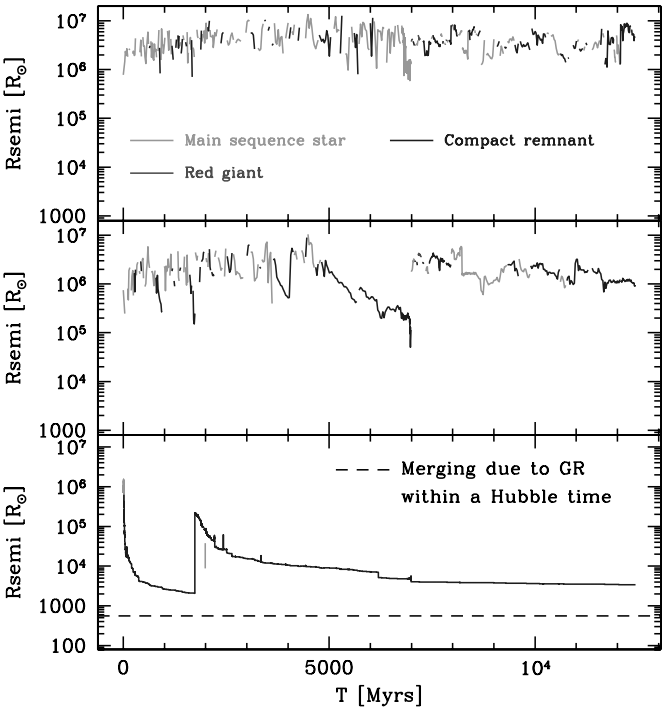

FIG. 14.—Semimajor axis of the three stars most deeply bound to the IMBH as a function of time for the cluster with $N = 128$K stars and a high upper mass limit. The object most closely bound to the IMBH is almost always another BH, which is among the heaviest objects in the cluster. The other stars are too far away from the BH to undergo mass transfer. [*See the electronic edition of the Journal for a color version of this figure*.]

3.6. *Gravitational Radiation*

Figures 14 and 15 depict the semimajor axis of stars that are most deeply bound to the IMBH for the two clusters with $N = 128$K stars. The energy of the deepest bound star decreases quickly in the beginning when it still has many interactions with passing stars. When the semimajor axis becomes significantly smaller than that of other stars, interactions become rare and the energy change slows down considerably. In both clusters, the innermost star is among the heaviest stars in the cluster, and would be a BH with several tens of $M_\odot$ for a globular cluster with a reasonable IMF. The innermost star will therefore not transfer mass onto the IMBH. All other stars have semimajor axes of $R > 10^6\ R_\odot$, which is too far for mass transfer, even if some stars will move on strongly radial orbits.

The time for two BHs in orbit around each other to merge because of emission of gravitational radiation is equal to (Evans et al. 1987)

$$T_{\rm GR} = \frac{5}{256}\frac{a^4c^5}{G^3m_1m_2M}F^{-1}(e) = 14.4\ {\rm yr}\left(\frac{a}{R_\odot}\right)^4\left(\frac{m_1}{10^3\ M_\odot}\right)^{-1} \times\left(\frac{m_2}{10\ M_\odot}\right)^{-1}\left(\frac{M}{10^3\ M_\odot}\right)^{-1}F^{-1}(e), \quad (9)$$

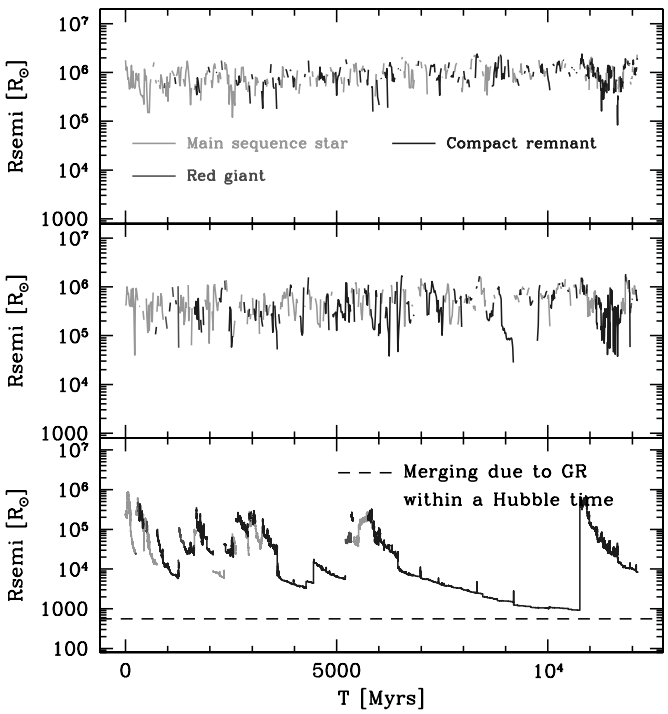

FIG. 15.—Same as Fig. 14, but for the case of a low upper mass limit. In this case, the star most closely bound to the IMBH is a high-mass white dwarf or neutron star. [*See the electronic edition of the Journal for a color version of this figure*.]

where a is the semimajor axis of the orbit, c is the speed of light, m_1 and m_2 are the masses of the two BHs, M is the combined mass, and F is a function of the orbital eccentricity e and is given by (Peters 1964)

$$F(e) = (1 - e^2)^{-7/2}\left[1 + (73/24)e^2 + (37/96)e^4\right]. \quad (10)$$

The eccentricity of the orbit of the innermost star fluctuates rapidly as long as the star undergoes many close encounters with passing stars, but becomes fairly stable as soon as the star has detached itself from the other cluster stars. Most of the time, the innermost stars moves on an orbit with moderate eccentricity and we can assume $e = 0.5$. With this value, the radius at which a BH of 20 $M_\odot$ merges with a 1000 $M_\odot$ IMBH within a Hubble time is $a = 562\ R_\odot$. This radius is marked by a dashed line in Figures 14 and 15. The semimajor axis for the innermost stars in our clusters are roughly a factor of 6 higher at the end of the simulation, so the merging timescale is around a thousand Hubble times, too long to have any noticeable effect on the orbits.

For a circular orbit, the frequency f and amplitude h of gravitational waves emitted by two BHs in orbit around each other at a distance R are given by (Douglas & Braginsky 1979)

$$f = \frac{1}{\pi}\sqrt{\frac{G(m_1 + m_2)}{a^3}} = 6.2\times10^{-3}\ \mathrm{Hz}\left(\frac{M}{10^3\ M_\odot}\right)^{1/2}\left(\frac{a}{R_\odot}\right)^{-3/2} \quad (11)$$

and

$$h = \sqrt{\frac{32}{5}}\frac{G^2 m_1 m_2}{c^4 a R} = 2.63\times10^{-18}\left(\frac{m_1}{10^3\ M_\odot}\right)\left(\frac{m_2}{10\ M_\odot}\right)\left(\frac{R}{\mathrm{kpc}}\right)^{-1}\left(\frac{a}{R_\odot}\right)^{-1}. \quad (12)$$

Figure 16 shows the amplitude and frequency of gravitational radiation emitted from the $N = 128$K clusters that started with a high upper mass limit. Each time the data were stored, we calculated both values, assuming that the cluster is at a distance of $R = 8$ kpc. The innermost BH is in too wide an orbit to be detectable.

How do these results change for globular clusters? In clusters with higher particle numbers, the distance of the innermost stars will be different. In Paper I it was shown that the energy generation rate in the cusp is proportional to

$$E_{\mathrm{cr}} \sim G^{3/2}\frac{m^3 n_0^2}{M_{\mathrm{BH}}^{-1/2}} \quad (13)$$

for an $\alpha = 1.75$ cusp. Such a profile should be established very close to the IMBH in higher N models. The rate at which energy can be transferred outward at the half-mass radius is given by

$$E_{\mathrm{tr}} \sim \frac{N_*(r_h)E_*(r_h)}{T_{\mathrm{Rel}}(r_h)} \sim \frac{M_{\mathrm{Cl}}^{1.5} m}{r_h^{2.5}} \quad (14)$$

if the weak N dependence in the Coulomb logarithm can be neglected. Since for a cluster evolving slowly along a sequence of equilibrium models energy generation must balance energy transport, a condition for n_0 can be obtained from both equations. The distances of the innermost stars from the IMBH in an $\alpha = 1.75$ cusp follow a relation $r_i \sim n_0^{-4/5}$. We therefore obtain for the distance of the innermost star from the IMBH

$$r_i \sim r_h \frac{m^{4/5}}{M_{\mathrm{Cl}}^{3/5} M_{\mathrm{BH}}^{1/5}}. \quad (15)$$

Using the relation found for r_h in § 3.1, $r_h \sim M_{\mathrm{Cl}}^{-1/3}$, we obtain for the dependence of r_i on the cluster mass M_{Cl}

$$r_i \sim M_{\mathrm{Cl}}^{-0.93}, \quad (16)$$

i.e., the distances of the innermost stars decrease almost linearly with the particle number. Assuming an $\alpha = 1.55$ cusp gives nearly the same scaling law. The data in our N-body runs is consistent with this relation. Equation (16) predicts that even in the most massive globular clusters, the distance of the innermost main-sequence stars from the IMBH is larger than $10^3\ R_\odot$, too large for stable mass transfer. Dynamical evolution alone is therefore not strong enough to form stable X-ray binaries involving the IMBH.

As Hopman et al. (2004) have shown, it might be possible for an IMBH to capture a passing star through tidal heating. In this case, the star could end up in a circular orbit with a small enough radius so that mass transfer onto the IMBH is possible. Encounters with passing stars will, however, scatter the star either out of the cusp or onto a highly eccentric orbit where it is disrupted by the IMBH. The present paper does not include orbital changes due to the tidal heating of stars, so detailed simulations have to be done to study the tidal capture rate of an IMBH and the further orbital evolution of the captured

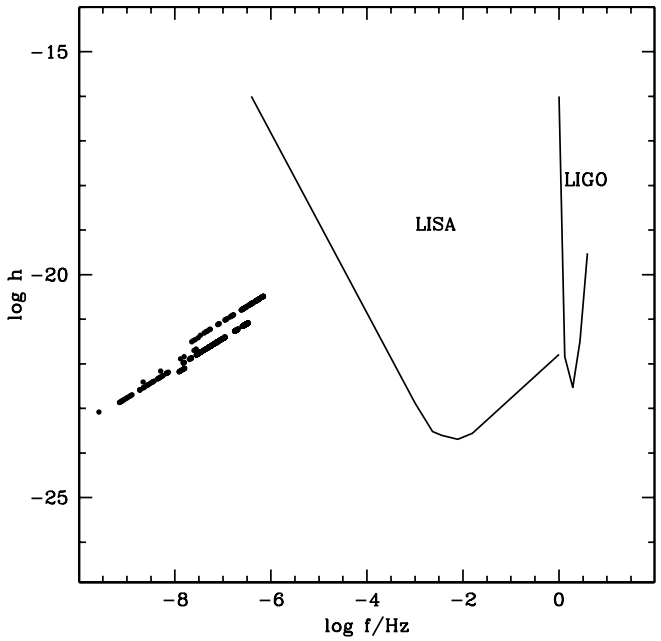

FIG. 16.—Frequency and amplitude of gravitational radiation emitted from the innermost BH binary for the $N = 128$K star cluster, which starts with a high upper mass limit. Although the binary hardens as a result of encounters with passing stars, the orbital separation is still too large, and hence the frequency too small, for the binary to become detectable.

stars. Apart from stars, the IMBH could also accrete cluster gas lost from post–main-sequence stars through stellar winds. The resulting X-ray flux depends on the gas fraction in the cluster and the details of the accretion mechanism, but could be bright enough to be observable under favorable conditions (Ho et al. 2003).

The situation looks more promising for gravitational radiation. A factor of 10 increase in the particle number from our largest $N = 128$K star runs would already be enough to form a tight IMBH-BH binary that merges within a Hubble time. If the semimajor axis of a 10–1000 $M_\odot$ BH binary in a galactic globular cluster is less than ~50 $R_\odot$, it would become visible. By this time, the time remaining to final merging has dropped to 10^8 yr. Making the conservative assumption that each globular cluster with an IMBH goes only once through such a phase, and assuming that 10% of all Galactic globular clusters contain IMBHs, chances are around 10% that any Galactic globular cluster is currently emitting detectable amounts of gravitational radiation. If a gravitational wave source has a signal-to-noise ratio larger than 2, *LISA* will have an angular resolution of a few degrees, making it possible to identify the globular cluster containing the IMBH.

The detection is even more likely if we consider extragalactic globular clusters. When the semimajor axis has dropped to $a = 1\ R_\odot$, a $10–1000\ M_\odot$ BH binary would be bright enough to be visible to distances of $R \approx 1$ Gpc. Based on the Two-Degree Field (2dF) galaxy redshift survey, Norberg et al. (2002) estimated a luminosity density of $\rho_L = (1.8 \pm 0.17) \times 10^8\ L_\odot\ \mathrm{Mpc}^{-3}$ at $z = 0$, which corresponds to roughly 0.1 Milky Way–sized galaxies every Mpc^{-3}. Assuming that each of them contains 100 globular clusters gives 5×10^{10} globular clusters inside 1 Gpc. Assuming again that 10% of all globular clusters contain an IMBH and that the merging rate of BHs with the central IMBH is constant over time gives five events that would be visible with *LISA* at any given time. Globular clusters containing IMBHs will therefore be an important source of gravitational wave emission from star clusters, in addition to double compact stars (Benacquista et al. 2001).

4. CONCLUSIONS

We have performed a set of large N-body simulations of multimass star clusters containing intermediate-mass black holes. Our simulations include a realistic mass spectrum of cluster stars, mass loss due to stellar evolution, two-body relaxation, and tidal disruption of stars by the central BH. These simulations are the first fully self-consistent simulations of realistic star clusters with IMBHs.

Our results can be summarized as follows. A density cusp forms around the central BH with a density profile $\rho \sim r^{-1.55}$ in three dimensions. For low-mass IMBHs with a mass less than a few percent of the cluster mass, the cusp extends out to a radius where the velocity dispersion in the core becomes comparable to the circular velocity of stars around the BH. In this case, the stars in the cusp contain only a fraction of the mass of the central BH, which makes the direct detection of the cusp difficult for IMBHs of $M_{\mathrm{BH}} \leq 1000\ M_\odot$. Globular clusters with IMBHs following the relation found by Gebhardt et al. (2000) for galactic bulges belong to this category. Only more massive BHs create a power-law cusp profile throughout the cluster core that would be directly visible.

When viewed in projection, the luminosity profiles of clusters with massive BHs display a constant density core. The presence of IMBHs in Galactic core-collapse clusters such as M15 is therefore ruled out unless these clusters have a stellar mass distribution very different from our clusters. As was shown in Baumgardt et al. (2003a), a more natural explanation for mass-to-light ratios that increase toward the center in such clusters is a dense concentration of neutron stars, white dwarfs, and stellar-mass BHs. The amount of mass segregation in a cluster with an IMBH is also smaller compared to a post–core-collapse cluster, the average mass of stars in the center being about $m = 0.6\ M_\odot$. Clusters with IMBHs therefore resemble star clusters that are in the precollapse phase also in terms of the amount of mass segregation.

All clusters with IMBHs expand because of close encounters of stars in the cusp around the central BH. We find that the values of the half-mass radii reached depend on the mass of the central BH and the number of cluster stars, but are nearly independent of the initial cluster radius and density profile. Portegies Zwart et al. (2004) have shown that central densities of more than $10^6\ M_\odot\ \mathrm{pc}^{-3}$ are necessary to form an IMBH through runaway merging of massive main-sequence stars. Similarly high densities are necessary to form an IMBH through the merging of stellar-mass BHs through gravitational radiation (Mouri & Taniguchi 2002). Such densities are among the highest found in globular clusters. Our simulations show that even if clusters with IMBHs start with very high densities, the subsequent cluster expansion is sufficient to put them among the least concentrated clusters after a Hubble time. Low-mass clusters surrounded by a strong tidal field will dissolve because of the cluster expansion, releasing their IMBHs. For clusters close enough to a galactic center, these IMBHs could then spiral into the center and merge through the emission of gravitational radiation. If enough IMBHs are formed, this process might provide the seed BHs for the supermassive BHs observed in galactic centers (Ebisuzaki et al. 2001).

IMBHs in star clusters disrupt mainly main-sequence stars and giants, with white dwarfs accounting for only 10% of all disruptions. In young star clusters, the tidal disruption rate of giants is similar to that of main-sequence stars. During our simulations, no neutron stars were disrupted, so IMBHs in star clusters do not emit gamma rays or gravitational radiation from such events. Most stars that were disrupted moved around the central BH on highly eccentric orbits with large semimajor axes. Even if 100% of the mass from disrupted stars is being accreted onto the central BH, tidal disruptions of stars are too rare to form an IMBH out of a $M_{\mathrm{BH}} \sim 50\ M_\odot$ progenitor, except if the initial cluster was significantly more concentrated than present-day globular clusters. In such cases, the density would, however, also be high enough that runaway merging of high-mass main-sequence stars would lead directly to the formation of an IMBH. The largest disruption rates for globular clusters that do not have core-collapse profiles are $\sim 10^{-7}\ \mathrm{yr}^{-1}$ for clusters with half-mass radii significantly smaller than predicted by our runs. Clusters with half-mass radii in agreement with our simulations have disruption rates that are 2 orders of magnitudes smaller. The BHs in such clusters are therefore inactive for most of the time.

The detection of a $1000\ M_\odot$ IMBH in a globular cluster through the measurement of radial velocities or proper motions of cluster stars requires the observation of about 20 stars in the central cusp. For globular clusters that are close enough, the central cusp extends to distances of several arcseconds, so the detection of an IMBH should be possible by either radial velocity or proper motion studies with *HST*.

BHs with masses of $5\ M_\odot$ or higher are strongly depleted in star clusters with IMBHs, since they sink into the center

through dynamical friction and then remove each other by close encounters in the central cusp around the IMBH (Kulkarni et al. 1993). Based on our simulations, we expect that only one high-mass BH remains in the cluster. This BH is among the heaviest BHs formed and ends up as the object most tightly bound to the IMBH. In our runs, the distance of the innermost BH to the IMBH was never small enough that the frequency of gravitational radiation was in the range observable for, e.g., *LISA*. For higher particle numbers or for clusters that start off more concentrated, it seems likely that a tight enough BH-IMBH binary is formed dynamically. If 10% of all globular clusters contain IMBHs and each IMBH merges with a stellar-mass BH at least once within a Hubble time, the chance that any Galactic globular cluster currently has a tight enough BH-IMBH binary to be detectable by *LISA* is 10%. Within a radius $R = 1$ Gpc, about five globular clusters would harbor bright enough sources for *LISA* at any one time.

We are grateful to Sverre Aarseth for making the NBODY4 code available to us and for his constant help with the program. We also thank Piet Hut, Marc Freitag, and Simon Portegies Zwart for useful comments. We finally thank the referee, Fred Rasio, for a careful reading of the manuscript and comments that led to an improvement of the paper.

REFERENCES

Aarseth, S. J. 1999, PASP, 111, 1333
Bahcall, J. N., & Wolf, R. A. 1976, ApJ, 209, 214
———. 1977, ApJ, 216, 883
Baumgardt, H., & Makino, J. 2003, MNRAS, 340, 227
Baumgardt, H., Makino, J., & Ebisuzaki, T. 2004, ApJ, 613, 1133
Baumgardt, H., et al. 2003a, ApJ, 582, L21
———. 2003b, ApJ, 589, L25
Benacquista, M. J., Portegies Zwart, S., & Rasio, F. A. 2001, Classical Quantum Gravity, 18, 4025
Binney, J., & Tremaine, S. 1987, Galactic Dynamics (Princeton: Princeton Univ. Press)
Cohn, H., & Kulsrud, R. M. 1978, ApJ, 226, 1087
Colpi, M., Mapelli, M., & Possenti, A. 2003, ApJ, 599, 1260
Douglas, D. H., & Braginsky, V. G. 1979, in General Relativity: An Einstein Centenary Survey, ed. S. W. Hawking & W. Israel (Cambridge: Cambridge Univ. Press), 30
Drukier, G. A., & Bailyn, C. D. 2003, ApJ, 597, L125
Ebisuzaki, T., et al. 2001, ApJ, 562, L19
Evans, C. R., Iben, I., & Smarr, L. 1987, ApJ, 323, 129
Ferraro, F. R., et al. 2003, ApJ, 595, 179
Frank, J., & Rees, M. J. 1976, MNRAS, 176, 633
Fregeau, J. M., Gürkan, M. A., Joshi, K. J., & Rasio, F. A. 2003, ApJ, 593, 772
Fryer, C. L., & Kalogera, V. 2001, ApJ, 554, 548
Gebhardt, K., Rich, R. M., & Ho, L. C. 2002, ApJ, 578, L41
Gebhardt, K., et al. 2000, ApJ, 539, L13
Gerssen, J., van der Marel, R. P., Gebhardt, K., Guhathakurta, P., Peterson R. C., & Pryor, C. 2002, AJ, 124, 3270
Gerssen, J., et al. 2003, AJ, 125, 376
Gürkan, M. A., Freitag, M., & Rasio, F. A. 2004, ApJ, 604, 632
Harris, W. E. 1996, AJ, 112, 1487
Heger, A., et al. 2003, ApJ, 591, 288
Ho, L. C., Terashima, Y., & Okajima, T. 2003, ApJ, 587, L35
Hopman, C., Portegies Zwart, S., & Alexander, T. 2004, ApJ, 604, L101
Hurley, J. R., Pols, O. R., & Tout, C. A. 2000, MNRAS, 315, 543
Kaaret, P., et al. 2001, MNRAS, 321, L29
Kawakatu, N., & Umemura, M. 2004, in ASP Conf. Ser., Proc. 25th Meeting of the IAU, Joint Discussion 11, Dynamics and Evolution of Dense Stellar Systems, ed. O. Engvold (San Francisco: ASP), in press
Kochanek, C. S. 1992, ApJ, 385, 604
Kroupa, P. 2001, MNRAS, 322, 231
Kulkarni, S. R., Hut, P., & McMillan, S. L. W. 1993, Nature, 364, 421
Lugger, P. M., Cohn, H. N., & Grindlay, J. E. 1995, ApJ, 439, 191
Makino, J., Fukushige, T., Koga, M., & Namura, K. 2003, PASJ, 55, 1163
Makishima, K., et al., 2000, ApJ, 535, 632
Marchant, A. B., & Shapiro, S. L. 1980, ApJ, 239, 685
Matsumoto, H., et al. 2001, ApJ, 547, L25
McCrady, N., Gilbert, A. M., & Graham, J. R. 2003, ApJ, 596, 240
McNamara, B. J., Harrison, T. E., & Anderson, J. 2003, ApJ, 595, 187
McNamara, B. J., Harrison, T. E., & Baumgardt, H. 2004, ApJ, 602, 264
Miller, M. C., & Hamilton D. P. 2002, MNRAS, 330, 232
Mouri, H., & Taniguchi, Y. 2002, ApJ, 566, L17
Newell, B., Dacosta, G. S., & Norris, J. 1976, ApJ, 208, L55
Norberg, P., et al., 2002, MNRAS, 336, 907
Peters, P. C. 1964, Phys. Rev. B, 136, 1224
Portegies Zwart, S. F., Baumgardt, H., Hut, P., Makino, J., & McMillan, S. L. W. 2004, Nature, 428, 724
Portegies Zwart, S. F., & McMillan, S. L. W. 2002, ApJ, 576, 899
Pryor, C., & Meylan, G. 1993, in ASP Conf. Ser. 50, Structure and Dynamics of Globular Clusters, ed. S. Djorgovski & G. Meylan (San Francisco: ASP), 357
Rasio, F. A., Freitag, M., & Gürkan, M. A. 2004, in Coevolution of Black Holes and Galaxies, ed. L. C. Ho (Cambridge: Cambridge Univ. Press), 138
Spitzer, L., Jr. 1969, ApJ, 158, L139
———. 1987, Dynamical Evolution of Globular Clusters (Princeton: Princeton Univ. Press)
Strohmayer, T. E., & Mushotzky, R. F. 2003, ApJ, 586, L61
Tremaine, S., et al. 1994, AJ, 107, 634